INFORMATION PROCESSING AT UNSTABLE EQUILIBRIUM POINTS IN THE RESTRICTED THREE BODY PROBLEM

Dylan R. Boone(1) **and Daniel J. Scheeres**(2)

(1)*Jet Propulsion Laboratory, 4800 Oak Grove Dr, Pasadena CA, 91109, 818-393-2844, dylan.boone@jpl.nasa.gov*

(2)*A. Richard Seebass Chair, Professor, University of Colorado at Boulder, 439 UCB, Boulder CO, 80309*

Abstract: *Information accumulation in the orbit determination process is affected by the structure of the State Transition Matrix (STM) which is used to map measurements in time. The STM can be decomposed into matrices of eigenvalues and eigenvectors which characterize the stability of a fixed point in the Restricted Three-body Problem as stable or unstable manifolds. Information from measurements is preferentially compressed or expanded along the directions of the stable or unstable manifolds based on whether the filtering formulation is current time or epoch state in the orbit determination process. The L_2 point in the Jupiter-Europa system is examined as a numerical example using range-rate measurement partials.*

Keywords: *Cassini, Titan, atmospheric density, navigation, orbit determination.*

1. Introduction

This work investigates the properties of phase space in the vicinity of an equilibrium point in the Restricted Three Body Problem and examines the time evolution of an equilibrium point orbiter's position-velocity covariance matrix. A mathematical development of information accumulation in the orbit determination process is given using the eigenstructure decomposition of the State Transition Matrix (STM). This decomposition involves matrices of right eigenvectors, eigenvalues, and left eigenvectors. The computed stable and unstable manifolds of an unstable fixed point, of which the Lagrange equilibrium points in the Restricted Three Body Problem are an example, are shown to affect the accumulation of information in the orbit determination process. Information is preferentially accumulated along the left unstable manifold direction for measurements mapped to epoch and along the left stable manifold direction for measurements mapped to the current state. This asymmetry in information mapping is due to the orthogonality of left and right eigenvectors. For epoch state filtering, the left unstable direction is best known and the right stable direction is least known. For a current state filter, the left stable direction is best known and the right unstable direction is least known. Analytical examples show this effect by decomposing the State Transition Matrix into its matrix exponential form.

A numerical simulation of trajectories in the vicinity of an equilibrium point shows that the covariance matrix collapses along preferred directions in phase space based on the properties of the State Transition Matrix. Trajectories in the Restricted Three Body Problem are drawn from a spherical covariance matrix about an equilibrium point in a Monte Carlo simulation and projected onto the plane of intersection of the stable and unstable manifolds of the equilibrium point. The Jupiter-Europa L2 equilibrium point is taken as a numerical example. The concept of manifold coordinates [1] reveals what components of the dispersed orbit initial conditions are aligned with the stable, unstable, and center manifolds associated with the equilibrium point, respectively. Simulations using a current state and an epoch state square-root information filter are presented and compared. The covariance matrix of an orbiter in the vicinity of an unstable fixed point collapses in preferential directions in phase space based on whether a current state or epoch state filter is used. This effect can be utilized for planning tracking schedules of a spacecraft and conducting covariance analysis of desired parameters to be estimated in the orbit determination process.

2. Jupiter-Europa system model

The specific astrodynamic problem under consideration is the Restricted Three Body Problem (RTBP) at the Jupiter-Europa system [2]. Jupiter and Europa are assumed to be in orbits about their mutual center of mass. The $\hat{x}$ direction points away from Jupiter's initial position on the Jupiter-Europa line, the $\hat{z}$ direction is aligned with the Europa's angular momentum vector, and the $\hat{y}$ direction completes a right-handed coordinate system. A coordinate transformation is used to shift the origin of the coordinate system from the barycenter to Europa's center of mass. The equations of motion are non-dimensionalized using the length and time units given in Table 1.

$$\ddot{\boldsymbol{r}} = -\mu_J \frac{\boldsymbol{r}-\boldsymbol{R}_{EJ}}{|\boldsymbol{r}-\boldsymbol{R}_{EJ}|^3} - \mu_J \frac{\boldsymbol{R}_{EJ}}{|\boldsymbol{R}_{EJ}|^3} - \mu_E \frac{\boldsymbol{r}}{|\boldsymbol{r}|^3} - 2n_S\hat{z}\times\dot{\boldsymbol{r}} - n_S\hat{z}\times(n_S\hat{z}\times\boldsymbol{r}) \tag{1}$$

Table 1: Europa parameters

Parameter	Value
n_S	$2.0483 \cdot 10^{-5}$ rad/s
LU	670900 km
TU	48822 s
μ_E	3202.7 km^3/s^2
μ_J	$1.2668 \cdot 10^8$ km^3/s^2

3. Europa Libration Points

For Europa, the reduced mass describing the three body system is $\mu = 2.52802 \cdot 10^{-5}$. To find the locations of the collinear libration points, the x scalar equation of motion is solved, with time derivatives set to zero along with the y and z coordinates set to zero. The roots of Equation 2 yield the locations of Europa's L_1, L_2, and L_3 points.

$$(x+1-\mu) - (1-\mu)\frac{x+1}{|x+1|^3} - \mu\frac{x}{|x|^3} = 0 \tag{2}$$

The x coordinates of the collinear libration points are given in Table 2. A spacecraft placed at these locations with zero velocity will remain there indefinitely in the RTBP.

Table 2: Europa collinear libration point x coordinates

	x (km)
L_1	$-1.35593 \cdot 10^4$
L_2	$+1.37445 \cdot 10^4$
L_3	$-1.34179 \cdot 10^5$

Since the dynamics are identically zero at an equilibrium point, numerical integration is not necessary. The local dynamics are characterized by the STM which itself is integrated using the dynamic partials matrix A. However, the A matrix is constant since its values depend only on the orbiter position, and an eigenvector of the A matrix is also an eigenvector of the STM. There is a simple relationship between the eigenvalues σ of the A matrix and the eigenvalues λ of the STM.

$$\lambda_i = e^{\sigma_i t} \tag{3}$$

So, the eigenstructure of the L_2 equilibrium point is available from the analytical description of the A matrix. Equation 4 shows the components of the A matrix and Equation 5 gives the partials of the potential:

$$A = \begin{bmatrix} 0 & 0 & 1 & 0 \\ 0 & 0 & 0 & 1 \\ U_{xx} & U_{xy} & 0 & 2 \\ U_{yx} & U_{yy} & -2 & 0 \end{bmatrix} \tag{4}$$

$$\begin{aligned} U_{xx} &= 1 - \frac{1-\mu}{r_J^3} - \frac{\mu}{r_E^3} + 3(1-\mu)\frac{(x+1)^2}{r_J^5} + 3\mu\frac{x^2}{r_E^5} \\ U_{xy} = U_{yx} &= 3\mu\frac{xy}{r_E^5} + 3y(1-\mu)\frac{x+1}{r_J^5} \\ U_{yy} &= 1 - \frac{1-\mu}{r_J^3} - \frac{\mu}{r_E^3} + 3(1-\mu)\frac{y^2}{r_J^5} + 3\mu\frac{y^2}{r_E^5} \end{aligned} \tag{5}$$

The eigenvectors and eigenvalues are computed from this analytical A matrix using the *eig* command in Matlab. The eigenvalues σ of the A matrix are shown in Table 3 to illustrate the instability of L_2. One eigenvalue has magnitude greater than one, corresponding to the unstable manifold, one eigenvalue has magnitude less than zero, corresponding to the stable manifold, and the final two eigenvalues are a complex conjugate pair representing the center manifold.

Table 3: Eigenvalues of A matrix for Europa L_2

	Value
λ_u	2.46012
λ_s	-2.46012
λ_{c1}	$0+2.04233i$
λ_{c2}	$0-2.04233i$

A simplified range-rate model is used to explore the processing of information from measurement partials at this equilibrium point. For the time periods considered in this simulation, Earth's position vector is fixed along the $\hat{u}$ direction in the Jupiter-Europa system. Equation 6 shows the range-rate measurement as the dot product of the Earth range direction and the orbiter velocity where T_{RI} is the transformation from the rotating frame to inertial frame.

$$\dot{\rho} = \hat{u}\cdot\boldsymbol{v}_{EE} \quad = \quad \hat{u}\cdot\left[T_{RI}\left(\boldsymbol{v}_R + \boldsymbol{\omega}\times\boldsymbol{r}_R\right)\right] \tag{6}$$

For a spacecraft at an equilibrium point, the rotating frame velocity $\boldsymbol{v}_R$ is zero. Equation 7 shows the partial of the range-rate measurement with respect to the rotating frame position and velocity where $\bar{U}$ is the unity dyad and $\tilde{\boldsymbol{\omega}}$ is the cross product matrix of the system angular velocity.

$$\frac{\partial \dot{\rho}}{\partial\left(\boldsymbol{r}_R, \boldsymbol{v}_R\right)} = \hat{u} \cdot T_{RI}\left[\tilde{\boldsymbol{\omega}}\,\bar{U}\right] = [1\,0\,0]\begin{bmatrix}\cos(n_S t) & -\sin(n_S t)\\ \sin(n_S t) & \cos(n_S t)\end{bmatrix}\left[\tilde{\boldsymbol{\omega}}\,\bar{U}\right] \tag{7}$$

This results in a $1x4$ partial since the xy plane is used for the equilibrium point analysis.

$$\frac{\partial \dot{\rho}}{\partial\left(\boldsymbol{r}_R, \boldsymbol{v}_R\right)} = \left[-n_S \sin(n_S t) \; -n_S \cos(n_S t) \; \cos(n_S t) \; -\sin(n_S t)\right] \tag{8}$$

This range-rate measurement partial is accumulated in the SRIF in epoch and current state formulations to explore how the manifolds of the equilibrium point influence the resulting covariance matrix. The following section gives the mathematical basis for the expected behavior of mapped partials.

4. Influence of STM Structure on Information Matrix

In a batch formulation of the square-root information filter, the information matrix Λ is updated with each processed measurement via the measurement partials $\tilde{H}$ [3]. These measurement partials are mapped to the epoch state by means of the STM which is integrated along with the equations of motion. The update is as follows:

$$\Lambda' = \Lambda + \Phi^T\left(t, t_0\right)\tilde{H}^T\tilde{H}\Phi\left(t, t_0\right) \tag{9}$$

As discussed previously, the STM can be decomposed into a product of matrices of right eigenvectors, left eigenvectors, and a diagonal matrix of eigenvalues.

$$\Phi = [\boldsymbol{u}]\,\mathrm{diag}(\lambda)\left[\boldsymbol{v}^T\right] = \begin{bmatrix}\boldsymbol{u}_1 & \boldsymbol{u}_2 & \cdots & \boldsymbol{u}_n\end{bmatrix}\begin{bmatrix}\lambda_1 & & 0\\ & \ddots & \\ 0 & & \lambda_n\end{bmatrix}\begin{bmatrix}\boldsymbol{v}_1^T\\ \boldsymbol{v}_2^T\\ \vdots\\ \boldsymbol{v}_n^T\end{bmatrix} \tag{10}$$

A range-rate measurement partial is decomposed into components along the left eigenvectors of the STM since these vectors span the measurement space. Using a summation to represent the different eigenvector contributions to the partial:

$$\tilde{H} = \frac{\partial \dot{\rho}}{\partial\left(\boldsymbol{r}_R, \boldsymbol{v}_R\right)} = \sum_i^N \alpha_i \boldsymbol{v}_i^T \tag{11}$$

Decomposing the STM and the measurement partials using the eigenvalues and eigenvectors gives the information matrix update equation in this form:

$$\Lambda' = \Lambda + \sum_i^N [\boldsymbol{v}]\,\mathrm{diag}(\lambda)\left[\boldsymbol{u}^T\right]\left(\alpha_i \boldsymbol{v}_i\right)\left(\alpha_i \boldsymbol{v}_i^T\right)[\boldsymbol{u}]\,\mathrm{diag}(\lambda)\left[\boldsymbol{v}^T\right] \tag{12}$$

where $[\boldsymbol{u}]$ is a matrix of right eigenvectors and $[\boldsymbol{v}]$ is a matrix of left eigenvectors. Using the properties of left and right eigenvectors, this update relationship can be simplified. The dot product of a left eigenvector and right eigenvector is zero unless their indices are equal. In other words, all left and right eigenvectors are orthogonal to one another except for those paired with the same eigenvalue.

$$\boldsymbol{v}_i \cdot \boldsymbol{u}_j = \begin{cases} 1, & \text{if } i = j. \\ 0, & i \neq j. \end{cases} \tag{13}$$

Using this property, only the eigenvector(s) aligned with the particular measurement partial will contribute to the addition to the information matrix. The left eigenvectors which make up the measurement partial will select out only their paired right eigenvectors and will dot to zero with all other STM eigenvectors. Using the matrix exponential form of the STM, where σ_i is the eigenvalue of the dynamics partials matrix A corresponding to λ_i:

$$\Lambda' = \Lambda + \sum_i^N \boldsymbol{v}_i e^{\sigma_i t} \left(\alpha_i \boldsymbol{u}_i^T \boldsymbol{v}_i\right) \left(\alpha_i \boldsymbol{v}_i^T \boldsymbol{u}_i\right) e^{\sigma_i t} \boldsymbol{v}_i^T \tag{14}$$

$$= \Lambda + \sum_i^N \alpha_i^2 e^{2\sigma_i t} \boldsymbol{v}_i \boldsymbol{v}_i^T \tag{15}$$

Since the batch formulation of the SRIF references the epoch time, all subsequent measurements will be mapped backward in time. Mapping backward in time along the unstable manifold is expected to decrease uncertainty or increase information content, the opposite of mapping forward in time [4]. Assume the measurement partial in Equation 15 is aligned with the unstable left eigenvector, which has a positive real eigenvalue λ greater than one. The natural logarithm of $\lambda_u > 1$ is positive and the measurements aligned with the unstable manifold direction will be mapped according to the exponential $e^{\sigma_u t}$. This will result in an increase in the amount of information in Λ along the left unstable manifold direction greater than any other direction since the exponential mapping will be greatest for the $\lambda_u > 1$ component. Correspondingly, the amount of information increase along the stable manifold direction will be less due to the stable eigenvalue λ_s being less than one. A series of measurements such as range-rate should sample across phase space and not predominantly align with any particular eigenvector. It is not as clear what the effect of STM mapping would be on measurements aligned with a right eigenvector. Returning to Equation 12, if the measurement partial is replaced with right eigenvector components:

$$\Lambda' = \Lambda + \sum_i^N [\boldsymbol{v}] \operatorname{diag}(\lambda) \left[\boldsymbol{u}^T\right] \left(\alpha_i \boldsymbol{u}_i\right) \left(\alpha_i \boldsymbol{u}_i^T\right) [\boldsymbol{u}] \operatorname{diag}(\lambda) \left[\boldsymbol{v}^T\right] \tag{16}$$

In this case, the orthogonality properties of left and right eigenvector properties do not simplify the analysis. The measurement partial will generally have nonzero dot products with all of the right eigenvectors in the $[\boldsymbol{u}]$ matrix portion of the STM, leaving no clear direction for enhanced information accumulation.

An analogous result comes out of the mathematics for current state measurement accumulation. In this case, the information matrix is mapped in time between measurement updates. Accumulating a measurement at epoch with no a priori information and then mapping to the next measurement time gives the following, where the mapping relation for the information matrix is the inverse of that for the covariance matrix:

$$\Lambda' = \Phi^{-T}\tilde{H}^T\tilde{H}\Phi^{-1} \tag{17}$$

Due to the definition of the STM and the properties of left and right eigenvectors discussed earlier, the inverse of the STM can be expressed as:

$$\Phi^{-1} = [\boldsymbol{u}]\,\mathrm{diag}(e^{-\sigma t})\left[\boldsymbol{v}^T\right] \tag{18}$$

such that the mapped information matrix becomes:

$$\Lambda' = [\boldsymbol{v}]\,\mathrm{diag}(e^{-\sigma t})\left[\boldsymbol{u}^T\right]\tilde{H}^T\tilde{H}\,[\boldsymbol{u}]\,\mathrm{diag}(e^{-\sigma t})\left[\boldsymbol{v}^T\right] \tag{19}$$

Since the inverse of the STM is used in mapping the information matrix between update times, the exponential controlling the mapping has a negative sign. This effectively reverses the trends for information accumulation discussed for the epoch state case. If a measurement partial aligned with a left eigenvector is substituted for $\tilde{H}$ in Equation 19, the exponential term associated with that eigenvector will have $\sigma > 0$ for the unstable direction or $\sigma < 0$ for the unstable direction. With the negative sign present in the mapping exponential, the left stable direction will accumulate information and reduce uncertainty more than the unstable direction. Again, due to the overall structure of the STM, measurement partials aligned with right eigenvectors do not produce any definite trends for information accumulation. This mapping effect of the STM is expected to dominate the overall shape of the covariance with respect to the left stable and unstable manifolds. In the following section, experiments are performed to test this hypothesis.

5. Covariance Evolution

This section investigates how the covariance accumulated from a series of range-rate measurement partials at the Europa L_2 point evolves in time. The range-rate partial developed in Equation 8 is used here. In general, this partial will have projections on to both the left and right eigenvectors. Both the epoch state and current state formulations of a SRIF are used to generate the covariance. A spherical a priori covariance of $1000 \cdot I_{4x4}$ is used for both cases. The focus here is on the evolution of the covariance relative to the manifolds rather than a numerical value. The left and right stable and unstable manifolds are computed for Europa L_2 and the covariance is projected into the plane of intersection of the left stable and unstable manifolds as described in Boone and Scheeres [5].

5.1. Epoch State Mapping

Starting from a spherical a priori covariance, range-rate measurement partials are accumulated at the Europa L_2 equilibrium point and an epoch covariance is computed. Partials are accumulated every 10 minutes and an epoch covariance matrix is computed using a SRIF at every time step.

Dispersions around the equilibrium point are drawn from the covariance matrix 10000 times and decomposed into manifold coordinates. The mathematics involving the manifold structure of the STM suggest that there will be reduced uncertainty in this covariance draw along the left unstable manifold direction. In the plots, the left manifolds are plotted as dotted lines and the right manifolds are plotted as solid lines. The stable directions are shown in green and the unstable directions are shown in red. The blue dots each represent one trajectory in the vicinity of the equilibrium points drawn from the covariance. In this way, the relative alignment of the covariance with any particular manifold can be seen.

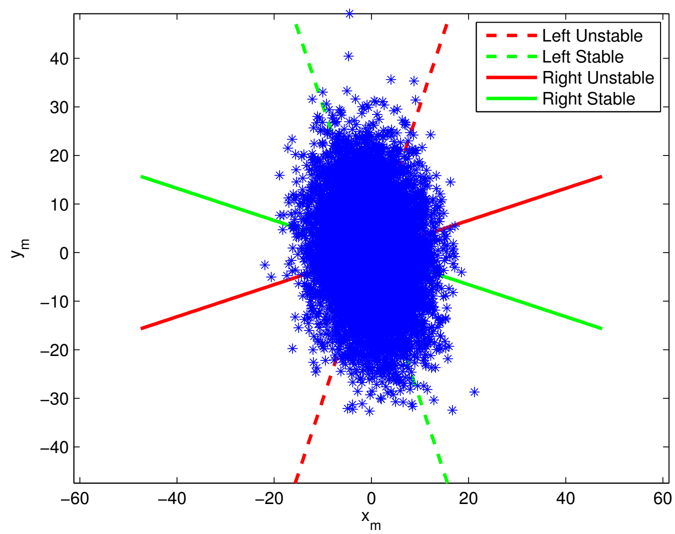

Figure 1: Epoch state covariance at $t = 10$ min

For epoch accumulation, the times given in the figures represent the last time a measurement partial was accumulated into the information matrix. The specific times shown are chosen for comparison between epoch and current state formulations. All partials are mapped to epoch using the STM. After one measurement partial, the covariance distribution is still nearly spherical as shown in Figure 1. After more partials are accumulated, the covariance starts to take on an orientation with the long axis slightly aligned with the right stable manifold as in Figure 2. At $t = 300$ minutes in Figure 3, the covariance is definitely compressed along the left unstable manifold and has its greatest extent along the right stable manifold.

As the mapping time increases, the effect of the unstable eigenvalue becomes more and more important. Continuing to accumulate partials stretches the covariance even more along the right stable manifold and compresses most along the left unstable direction. Since Earth follows a cyclic pattern in the range-rate model, all eigenvectors of the STM should be sampled equally in this covariance computation. However, the results verify the prediction that the left unstable eigenvector will have the most influence on the epoch covariance. This makes intuitive sense as any errors along the right stable manifold direction would be expected to contract when mapped forward in time. With the measurement partials being mapped backward in time for the epoch covariance, errors along the right stable manifold are expanded.

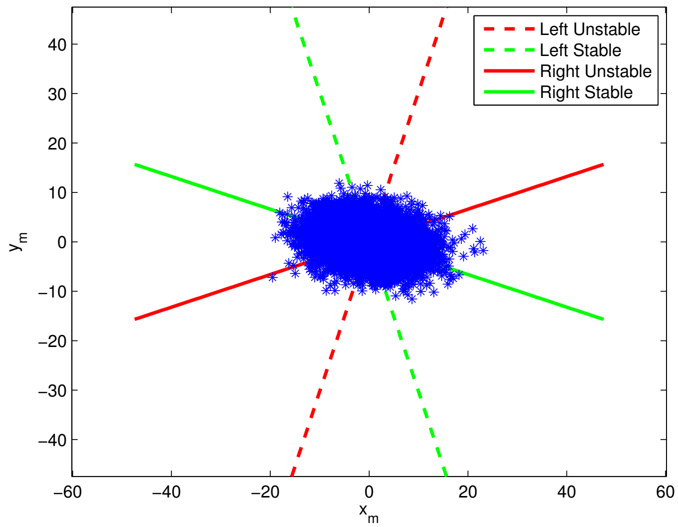

Figure 2: Epoch state covariance at $t = 50$ min

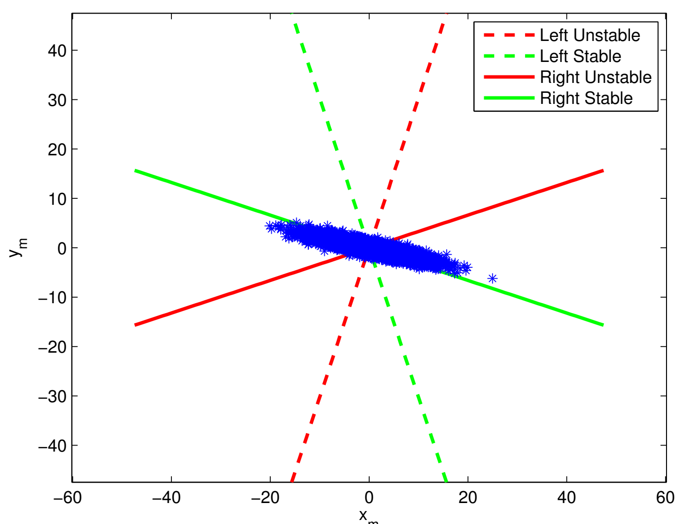

Figure 3: Epoch state covariance at $t = 300$ min

5.2. Current State Mapping

Starting from a spherical a priori covariance, range-rate measurement partials are accumulated at the Europa L_2 equilibrium point and a current state covariance is computed. Partials are accumulated every 10 minutes and the covariance matrix is computed using a current state SRIF.

Dispersions around the equilibrium point are drawn from the covariance matrix 10000 times and decomposed into manifold coordinates. For the current state formulation, the mathematics involving the manifold structure of the STM suggest that there will be reduced uncertainty in this covariance draw along the left stable manifold direction. Figure 4 shows the covariance decomposition after

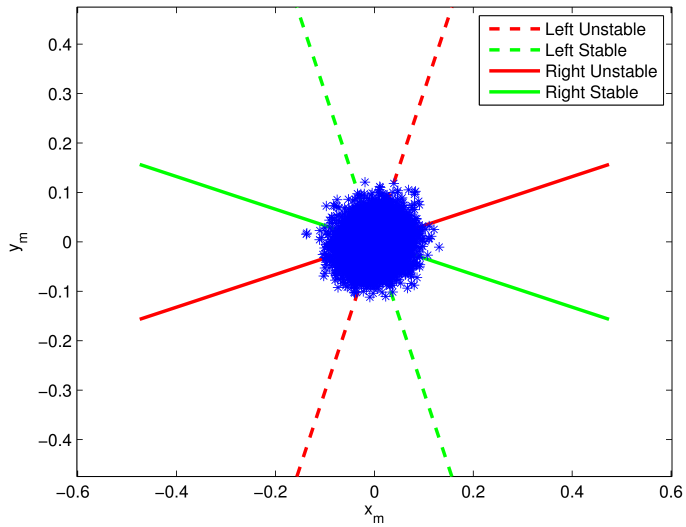

Figure 4: Current state covariance at $t = 10$ min

a single measurement has been taken at $t = 10$ minutes. The distribution is still spherical, but compressed from the a priori since this measurement has not yet been mapped in any way. For the current state filter, the entire information matrix is mapped between updates and in this study there was no measurement at epoch.

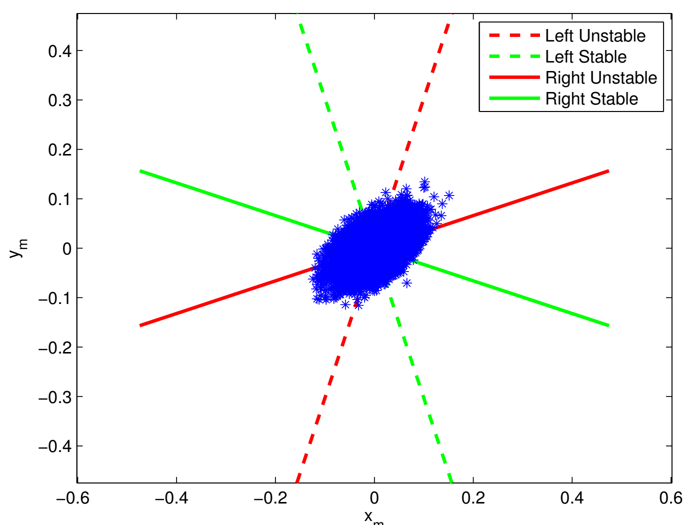

Figure 5: Current state covariance at $t = 50$ min

After mapping the covariance and accumulating additional measurements, the properties of the STM mapping begin to manifest in Figure 5. The distribution is no longer spherical and there is some compression along the left stable manifold direction. Each measurement partial adds information and reduces the volume of the uncertainty but the information matrix is also mapped in time between measurement updates, expanding along the direction of the right unstable manifold. This right unstable manifold controls evolution forward in time.

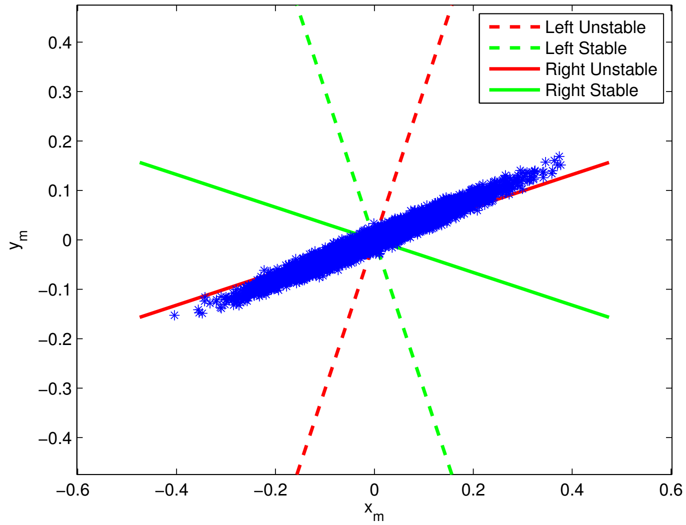

Figure 6: Current state covariance at $t = 300$ min

Figure 6 shows the covariance being stretched even more along the right unstable manifold and compressing along the left stable manifold. This confirms the mathematical prediction based on the structure of the STM mapping in the SRIF process. The reason for compression along the left stable manifold in this case is due to the negative sign imparted to the exponential mapping in the time update equation for the information matrix. Similar behavior would be expected for covariance analyses conducted around unstable periodic orbits since they possess stable and unstable manifolds. However, the manifold structure for periodic orbits would also have to be mapped in time. Numerical difficulties arise in mapping the manifolds of the monodromy matrix which controls the local dynamics around a periodic orbit. The angle between the stable and unstable manifolds would be constant at each point in the orbit although rotated in phase space. This is difficult to enforce numerically when many applications of the STM would be required for manifold decomposition at many measurement times. A libration point was chosen for this study because of the constant manifold properties. Such a study for periodic orbits may be the subject of future work.

6. Conclusions and Future Work

The computed stable and unstable manifolds of an unstable fixed point, which includes the Lagrange equilibrium points in the RTBP, are shown to affect the accumulation of information in the orbit determination process. Information is preferentially accumulated along the left unstable manifold for measurements mapped to epoch and along the left stable manifold for covariances mapped to the current state. This is due to the orthogonality of left and right eigenvectors and the eigenstructure of the STM, which can be decomposed into matrices of right eigenvectors, eigenvalues, and left eigenvectors. An asymmetry in information mapping is shown between left and right eigenvectors.

The information mapping theory can be applied to specific real measurements such as a position measurement along a given direction. If that direction is perpendicular in phase space to the eigenvector describing a left manifold, there will be a deficient phase space direction in the paired right manifold direction. Also, a particular direction or measurement schedule could be developed to gain the most information on the estimated state from the smallest number of measurements. Depending on the type of estimation, taking measurements where the partial is aligned with the left stable or unstable manifolds can yield information compression. A full rank information matrix can be constructed from a series of the same measurement aligned with a right eigenvector. However, a series of measurements missing a left eigenvectors will have a deficient measurement direction along the right eigenvector paired with the omitted left eigenvector. Future studies will focus on constructing measurements that have maximum contributions to the information matrix as well as developing a numerically stable method for mapping eigenvectors in time.

7. Acknowledgements

The authors would like to acknowledge the NASA Earth and Space Science Fellowship program for their support through grant number NNX11AP33H.

This work was done as a private venture and not in the author's capacity as an employee of the Jet Propulsion Laboratory, California Institute of Technology.

8. References

[1] Gustafson, E. and Scheeres, D. J. "Dynamically relevant local coordinates for halo orbits." "Astrodynamics Specialist Conference," AIAA 2008-6432. American Astronautical Society, 2008.

[2] Szebehely, V. Theory of Orbits: The Restricted Problem of Three Bodies. Academic Press, 1967.

[3] Tapley, B., B. Schutz and Born, G. Statistical Orbit Determination. Elsevier Academic Press, 2004.

[4] Scheeres, D. J. H. and Hou. "Influence of Unstable Manifolds on Orbit Uncertainty." Journal of Guidance, Control, and Dynamics, Vol. 24, No. 3, pp. 573–585, 2001.

[5] Boone, D. R. and Scheeres, D. J. "Long-life Europa Geodesy Orbits Accounting for Navigation Uncertainties." Journal of Guidance, Control, and Dynamics, Vol. 37, No. 2, pp. 413–424, 2014.